

## Anomalous photoluminescence in BaS:Eu

P. F. Smet,\* J. E. Van Haecke, F. Loncke, H. Vrielinck, F. Callens, and D. Poelman  
*Department of Solid State Sciences, Ghent University, Krijgslaan 281-S1, 9000 Gent, Belgium*  
 (Received 17 January 2006; revised manuscript received 16 May 2006; published 19 July 2006)

The photoluminescence emission properties of BaS:Eu powders have been studied. At room temperature, several weak emission bands related to impurities or intrinsic defects are observed in the visible part of the spectrum. The strongest emission band is situated mainly in the infrared with a peak emission wavelength of 878 nm and is related to  $\text{Eu}^{2+}$  centers. From the viewpoint of the large Stokes shift, the large emission bandwidth, and the temperature quenching profile, the  $\text{Eu}^{2+}$  emission in BaS:Eu is totally different than what can be expected from the analogy with the similar materials CaS:Eu and SrS:Eu. Hence the emission in BaS:Eu is anomalous. Photoluminescence excitation and electron paramagnetic resonance spectra show that the incorporation of  $\text{Eu}^{2+}$  in BaS is not radically different from SrS:Eu or CaS:Eu. The appearance of infrared emission is related to the position of the  $5d$  excited level of  $\text{Eu}^{2+}$  relative to the conduction band of BaS, which leads to autoionization of the  $\text{Eu}^{2+}$  centers upon  $4f^7-4f^65d$  excitation and the formation of impurity trapped excitons. The influence of trap levels was studied by thermoluminescence and a major trap with an activation energy of 0.51 eV was found. The thermal quenching behavior was evaluated as well.

DOI: 10.1103/PhysRevB.74.035207

PACS number(s): 78.60.-b, 78.55.-m, 76.30.Kg

### I. INTRODUCTION

In the large field of inorganic luminescence [including cathodoluminescence, thin film electroluminescence, and light-emitting diode (LED) color conversion], much effort is still being directed to the development of new phosphor materials. Amongst many, BaS has been studied as a host material for inorganic thin film electroluminescence. The reported dopant ions in BaS include copper, bismuth, manganese, and the rare earths cerium and europium.<sup>1-3</sup>

Recently, BaS:Eu has been used as a source material for several ternary and quaternary phosphors, e.g.,  $\text{BaAl}_2\text{S}_4:\text{Eu}$ ,  $\text{Ba}_{1-x}\text{Mg}_x\text{Al}_2\text{S}_4:\text{Eu}$ ,  $\text{BaGa}_2\text{S}_4:\text{Eu}$ , and  $\text{Ba}_2\text{SiS}_4:\text{Eu}$ .<sup>4,5</sup> Especially the blue-emitting  $\text{Ba}_{1-x}\text{Mg}_x\text{Al}_2\text{S}_4:\text{Eu}$  is currently in the picture as the best candidate for the commercial development of flat panel displays based on inorganic thin film electroluminescence (EL). Surprisingly, the luminescence of the europium-doped binary phosphor BaS itself is not very well known and contradictory claims about the emission properties have been made. First of all, this work aims at finally clarifying the emissive behavior of BaS:Eu from a fundamental point of view. Secondly, these data are very useful for the study of europium-doped ternary (and quaternary) thin films for which BaS is used as a source material. In general, the deposition of stoichiometric ternary sulfides is far from straightforward as specific deposition techniques are required, such as dual-source e-beam evaporation<sup>4</sup> or multi-source vapor deposition.<sup>6</sup> During postdeposition thermal annealing of such films, stoichiometric deviations can occur leading to trace amounts of separate phases, such as the starting binary sulfides.<sup>7</sup> Beside analysis techniques such as x-ray diffraction, studying the luminescence is often an appropriate and sensitive tool to identify the presence of trace amounts of the binary sulfides. In the case of BaS:Eu-based ternary materials, trace amounts in the synthesized material will remain undetected upon inspection of the visual luminescence, given the fact that the emission of BaS:Eu is almost entirely situated in the infrared, as will be shown in this work.

### II. LITERATURE REVIEW

#### A. $\text{Eu}^{2+}$ emission

Before giving a review of the available literature data on BaS:Eu powders and thin films, we briefly discuss the general emission mechanism of  $\text{Eu}^{2+}$  incorporated in a host material. Dorenbos formulated a general relationship for the energy difference between the lowest  $4f^m$  and the first  $4f^{m-1}5d^1$  level in divalent ( $Q=2+$ ) and trivalent ( $Q=3+$ ) lanthanide ions.<sup>8</sup> Applied to the case of  $\text{Eu}^{2+}$ , one can write for the energy of  $fd$  absorption in a host crystal  $A$ ,

$$E_{\text{abs}}(\text{Eu}^{2+}, A) = E_{A \text{ free}}(\text{Eu}^{2+}) - D(2+, A).$$

The value  $E_{A \text{ free}}(\text{Eu}^{2+})$  is the  $fd$  transition energy for the free (gaseous) ion and is rounded to  $34\,000 \text{ cm}^{-1}$ . The redshift  $D(2+, A)$  can be determined from any divalent lanthanide in the compound  $A$ . Shifting  $E_{\text{abs}}(\text{Eu}^{2+}, A)$  down with the Stokes shift  $\Delta S(2+, A)$  leads to the  $df$  emission energy

$$E_{\text{em}}(\text{Eu}^{2+}, A) = E_{A \text{ free}}(\text{Eu}^{2+}) - D(2+, A) - \Delta S(2+, A).$$

In most compounds (except for some specific oxides and fluorides),  $E_{\text{em}}(\text{Eu}^{2+}, A)$  is lower than the  $4f^7(^6P_{7/2})-4f^7(^8S_{7/2})$  transition energy. In that case,  $df$  broadband emission is observed instead of line emission in the wavelength range from 356 to 364 nm, typical for the  $ff$  transitions in  $\text{Eu}^{2+}$ . In the case of broadband emission, Dorenbos distinguishes two types: “normal” and “anomalous”  $df$  emission. In the first case, the emission arises from the electric dipole and spin-allowed transition between the relaxed  $4f^6(^7F_0)5d^1$  excited state and the  $4f^7(^8S_{7/2})$  ground state. This normal emission is observed in the majority of the 300  $\text{Eu}^{2+}$ -doped compounds compiled in Ref. 8. For these compounds, the most common Stokes shift is  $1350 \text{ cm}^{-1}$  and the emission bandwidth ( $\Gamma$ ) is about  $1600 \text{ cm}^{-1}$ . The anomalous emission is characterized by one or more of the following observations: a much larger Stokes shift [ $\Delta S(2+, A) > 4000 \text{ cm}^{-1}$ ], a much larger bandwidth ( $\Gamma > 3000 \text{ cm}^{-1}$ ), a deviant tempera-

TABLE I. Emission and the physical properties of europium-doped alkaline earth sulfides (compiled from Refs. 8, 11, and 12) with  $\Gamma$  the full width at half maximum of the emission band,  $D$  the redshift, and  $\Delta S$  the Stokes shift. The values of 10 Dq are from Ref. 11, while the values of 14 000  $\text{cm}^{-1}$ , 15 000  $\text{cm}^{-1}$ , and 12 000  $\text{cm}^{-1}$  are reported for, respectively, MgS, CaS, and SrS in Ref. 13, with an error margin of 2000  $\text{cm}^{-1}$ .

Compound	Cation radius (pm)	$\lambda_{\text{abs}}$ (nm)	$\lambda_{\text{em}}$ (nm)	10 Dq ( $\text{cm}^{-1}$ )	$\Gamma(\text{RT})$ ( $\text{cm}^{-1}$ )	$D(2+, A)$ ( $\text{cm}^{-1}$ )	$\Delta S(2+, A)$ ( $\text{cm}^{-1}$ )
MgS	65	562	592	19500	1120	16146 $\pm$ 400	902
CaS	99	600	652	18750	1460	17766 $\pm$ 925	1329
SrS	113	550	620	17400	1930	15706 $\pm$ 65	2223
BaS	135		572	16100	3200		

ture quenching and luminescence decay profile.<sup>9</sup> This type of emission is related to the autoionization of the  $\text{Eu}^{2+} 5d$  electron to the conduction band, which can be followed by trapping of the electron at impurities (including the ionized Eu ion). The anomalous emission is then the radiative return to the ground state of  $\text{Eu}^{2+}$  (Ref. 9). An explanation for this impurity-trapped exciton emission was first provided by McClure and Pedrini.<sup>10</sup>

For normal emission, the redshift  $D(2+, A)$  is determined by two major contributions: one arising from the crystal field splitting and one from the centroid shift. The latter is related to the covalency between the  $\text{Eu}^{2+} 5d$  orbital and the  $p$  orbitals of the ligand anions. The major contribution in the  $MS$  compounds (with  $M=\text{Mg, Ca, Sr, Ba}$ ) originates from the crystal field splitting, which is determined to first order by the first anion coordination polyhedron.

In Table I, the emission properties of the Eu-doped binary sulfides MgS, CaS, SrS, and BaS are shown. For the position of the emission maxima, the following trend is observed in the series from CaS to BaS: the larger the host cation, the smaller the crystal field splitting and the smaller the redshift (i.e., leading to emission at shorter wavelengths). For the mixed compounds  $\text{Ca}_{1-x}\text{Sr}_x\text{S}:\text{Eu}^{2+}$  this relationship holds as well, as the position of the emission maxima shifts almost linearly from 652 nm to 620 nm upon increasing  $x$  from 0 to 1 (Refs. 11 and 14). The exception in Table I is MgS, which shows an unexpected blueshift compared to CaS. However, in the mixed compounds  $\text{Mg}_x\text{Ca}_{1-x}\text{S}:\text{Eu}^{2+}$  the emission is redshifted to 658 nm at  $x=0.35$ , but starts to blueshift for higher  $x$  values.<sup>11</sup> This effect has been related to the stress the relatively large  $\text{Eu}^{2+}$  ion (ionic radius of 115 pm) experiences upon substitution for the much smaller  $\text{Mg}^{2+}$  ion (ionic radius of 65 pm).

### B. BaS:Eu<sup>2+</sup>

The limited data for BaS:Eu powder in Table I are based on Ref. 11, but have not been reproduced since then for powders (1984). Although the reported emission peak at 572 nm seems in line with the trend discussed above (the larger the cation, the shorter the emission wavelength), the full width at half maximum (FWHM) of the emission band is considerably larger for BaS (i.e., 3200  $\text{cm}^{-1}$ ) compared to SrS (1930  $\text{cm}^{-1}$ ) and CaS (1460  $\text{cm}^{-1}$ ). A completely different emission behavior, although not consistent, was found by several authors in BaS:Eu thin films.

Ihanus *et al.* reported the PL and EL emission spectra of BaS:Eu thin films prepared by atomic layer deposition.<sup>15</sup> The EL emission intensity was very low (4  $\text{cd}/\text{m}^2$  at 1 kHz, 40 V above threshold) and the emission was broadband, with a peak reported at 712 nm, although no corrections for the wavelength-dependent detector sensitivity were made to the recorded spectra.<sup>15</sup> No emission band was observed near 572 nm, nor any line emission originating from internal  $\text{Eu}^{3+}(4f^6)$  transitions. The PL emission spectrum was similar to the EL spectrum.

Maddix reported the EL properties of BaS:Eu thin films, prepared by electron-beam evaporation of BaS pellets and co-evaporation of EuS or  $\text{EuF}_3$  as a dopant source.<sup>16</sup> Using EuS, the EL emission spectrum was composed of an  $\text{Eu}^{3+}$  line emission superposed on a (relatively weak) broadband emission centered at about 600 nm. Using  $\text{EuF}_3$  as a dopant source, the emission spectrum almost entirely consisted of  $\text{Eu}^{3+}$  line emission. The formation of separate Eu complexes within the BaS host was mentioned to explain the presence of  $\text{Eu}^{3+}$  emission. Nevertheless, the “expected”  $\text{Eu}^{2+}$  broadband emission at 572 nm was not observed. It is interesting to note that Maddix also observed that BaS EL devices doped with Mn, Pb, Ag, and Sn all showed a weak and broadband emission peaking between 560 and 580 nm. Even an intentionally undoped device emitted at 560 nm, albeit very weakly. This emission band was then related to an intrinsic defect or a possible copper contamination. PL emission of BaS:Cu powders has indeed been studied, but is normally centered at 585 nm at room temperature.<sup>3</sup>

Recently, we reported the EL emission properties of BaS:Eu EL devices, prepared by electron-beam evaporation from  $\text{H}_2\text{S}$  sintered BaS:Eu pellets with different Eu concentration.<sup>17</sup> At relatively low dopant concentration (0.5 mol %), the EL emission spectrum was composed of a broad emission band extending into the infrared, and peaking at a wavelength of 740 nm (or longer, as at that time no suitable infrared-sensitive equipment was available for these measurements). Superposed were relatively weak  $\text{Eu}^{3+}$  emission lines. Higher Eu concentration (up to 5 mol %) led to an emission spectrum entirely composed of  $\text{Eu}^{3+}$  emission lines. Again, the emission band at 572 nm was not detected.

In order to establish the position of the  $\text{Eu}^{2+}$  emission band and more specifically to elucidate the mechanisms of emission in BaS:Eu we prepared powders with various doping concentrations, following two synthesis routes to check for technique-dependent contaminations. In the present paper

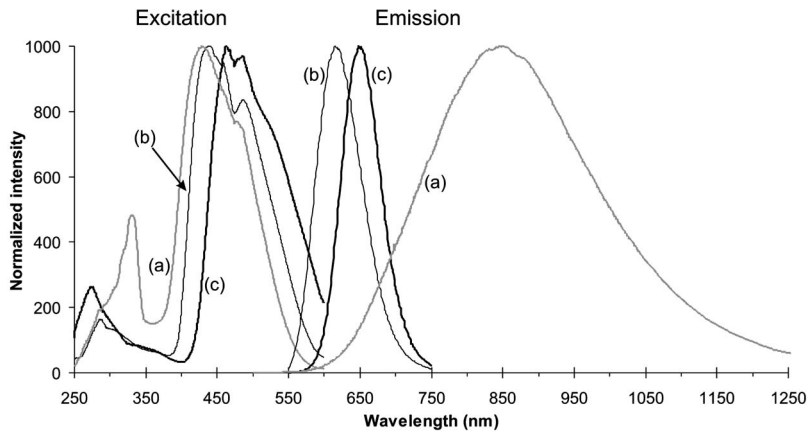


FIG. 1. Normalized emission and excitation spectra obtained at room temperature for (a) BaS:Eu[0.1%], (b) SrS:Eu[0.1%], and (c) CaS:Eu[0.1%] prepared by sintering. Excitation spectra were recorded at the peak emission wavelength. Emission spectra were obtained at 425, 445, and 465 nm for BaS:Eu, SrS:Eu, and CaS:Eu, respectively.

we report the PL emission and excitation characteristics of these powders and we relate them to the analogous systems CaS:Eu and SrS:Eu. In addition electron paramagnetic resonance (EPR) measurements have been performed on powders in order to obtain information on the location and the symmetry of the  $\text{Eu}^{2+}$  centers.

### III. EXPERIMENT

Two techniques were applied for the preparation of the CaS:Eu, SrS:Eu, and BaS:Eu powders. “Sintering” refers to a mixture of commercially available sulfides (CaS: 99.99%, CERAC; SrS: 99.9%, CERAC; BaS: 99.7% Alfa Aesar) and an appropriate amount of  $\text{EuF}_3$  (99.9%, CERAC) which is sintered at an elevated temperature (900 °C to 1000 °C) in a continuous flow of  $\text{H}_2\text{S}$  at atmospheric pressure. The “wet chemical synthesis” refers to a synthesis starting from alkaline earth salts [ $\text{Ba}(\text{NO}_3)_2$ , 99.95%, Alfa Aesar] and ammonium sulfate (99.95%, Alfa Aesar) as aqueous solutions. Details of this technique can be found in previous publications.<sup>14,18</sup> Dopant concentrations mentioned in this work are expressed in mol %, unless stated otherwise.

Steady state photoluminescent (PL) emission and excitation (PLE) spectra were recorded with a FS920 fluorescence spectrometer (Edinburgh Instruments), equipped with a Hamamatsu R928P red-sensitive photomultiplier (wavelength range from 200 to 850 nm) and a Ge infrared detector (700 to 1600 nm). All presented emission spectra have been corrected for the detector sensitivity by appropriate calibra-

tions. Spectrally resolved decay measurements were obtained with a pulsed nitrogen laser (337.1 nm, pulse length 800 ps, repetition rate 1 Hz) and a 1024-channel Intensified CCD (Andor Technology) attached to a 0.5 m Ebert monochromator. Low temperature and thermoluminescence measurements were performed using a cold-finger cryostat with liquid nitrogen. The temperature was monitored using a LakeShore Si diode (DT-470-CU-11).

EPR measurements were performed at room temperature in  $Q$ -band (34 GHz), using a Bruker Eleksys e500 spectrometer. The microwave power and modulation amplitude were set at 5 mW and 0.1 mT, respectively.

### IV. RESULTS

#### A. $\text{Eu}^{2+}$ emission and excitation spectra

Figure 1 shows emission spectra of CaS:Eu[0.1%], SrS:Eu[0.1%], and BaS:Eu[0.1%] powders prepared by sintering, measured at room temperature, upon excitation at 465, 445, and 425 nm, respectively, as well as excitation spectra at the peak emission wavelength. The wavelength of the emission maximum for CaS:Eu and SrS:Eu is in good correspondence with the literature data presented earlier (see Table II). The absorption wavelength ( $\lambda_{\text{abs}}$ ) in Table II refers to the peak wavelength for the lowest excitation level, being  ${}^7F_0$ . The typical staircase structure caused by the  $4f^6({}^7F_J)5d$  levels is, however, not fully resolved in the excitation spectra. The approximation proposed by Dorenbos to calculate

TABLE II. Emission properties of europium-doped alkaline earth sulfides as prepared by sintering in this work, with  $\Gamma$  the full width at half maximum of the emission band and  $\Delta S$  the Stokes shift. Data in parentheses refer to the literature data shown in Table I.  $\lambda_{\text{abs}}$  was determined according to the method described in Ref. 8.

Compound	$T$ (K)	Absorption		$\lambda_{\text{em}}$ (nm)	$\Gamma(\text{RT})$ ( $\text{cm}^{-1}$ )	$\Delta S(2+, A)$ ( $\text{cm}^{-1}$ )
		edge (eV) (Ref. 1)	$\lambda_{\text{abs}}$ (nm)			
CaS	293	4.20	603 (600)	653 (652)	1520 (1460)	1270 (1329)
SrS	293	4.12	561 (550)	620 (620)	1970 (1930)	1696 (2223)
BaS	293	3.49	546(-)	878 (572)	3980 (3200)	6925(-)
BaS	70		542(-)	938(-)	2660(-)	7790(-)

$\lambda_{\text{abs}}$  was used instead, which can lead to small errors for  $\lambda_{\text{abs}}$  and the therefrom calculated Stokes shift.<sup>8</sup>

For BaS:Eu, the emission spectrum is characterized by a broad emission band mainly situated in the near infrared, with an emission maximum at 878 nm. The position and width of this emission band does not depend on the dopant concentration in the studied range (0.1 to 1.0%) or on the preparation method (sintering or wet chemical synthesis). The emission band peaking at 572 nm, as reported by Kasano,<sup>11</sup> is not observed.

Figure 1 also shows the excitation spectrum corresponding to the BaS:Eu emission band. The similarity to the excitation spectra of CaS:Eu and SrS:Eu is striking, which relates the infrared emission bands in BaS:Eu unambiguously to transitions involving  $\text{Eu}^{2+}$  ions. The excitation bands for BaS:Eu in the wavelength range from 400 to 550 nm are clearly shifted towards shorter wavelength compared to those for SrS:Eu and CaS:Eu, which is indeed what one would expect on the basis of the lower value of the crystal field strength for BaS:Eu.

In the excitation spectra, two different contributions are observed:  $\text{Eu}^{2+}$  internal transitions and host excitation. The  $\text{Eu}^{2+} 4f^7-4f^65d^1$  absorption is situated in the visible part of the excitation spectrum. Due to the crystal field splitting, the 5d level is split in two levels  $t_{2g}$  and  $e_g$ . The transitions to the higher level  $e_g$  are masked by the band gap absorption. By comparing the absorption spectra of undoped CaS and SrS with excitation spectra for CaS:Eu and SrS:Eu, Yamashita already noticed that the  $e_g$  excitation band partially overlaps with the band gap absorption.<sup>12</sup> For BaS:Eu, having a smaller band gap (Table II) and a higher excitation energy compared to the former materials, only the excitation to the  $t_{2g}$  level is visible. While undoped BaS has a white to light gray body color, doping with Eu leads to an orange body color, due to absorption associated with the  $t_{2g}$  excitation band. The excitation below 340 nm is assigned to the band gap transition of the host material (Table II). Its structure is discussed in more detail in Section IV B.

Upon cooling to 70 K, the total emission intensity increases by a factor of about five, along with a shift to lower energy. From the Arrhenius plot (see the inset in Fig. 2) the activation energies of 14 meV (for the low temperature part) and 190 meV (in the temperature region above 200 K) were obtained. At 70 K the emission band is centered at 938 nm, with a FWHM of  $2660 \text{ cm}^{-1}$  (Fig. 2 and Table II). This behavior is unlike that of CaS:Eu or SrS:Eu, where the position of the emission band changes less than 5 nm when cooling from 300 to 6 K (Ref. 12). Furthermore, the latter materials hardly show any thermal quenching up to room temperature. While the luminescence decay profile of lightly doped CaS:Eu and SrS:Eu can normally be fitted with a single exponential over several orders of magnitude (with a time constant of 1.3 and 0.8  $\mu\text{s}$ , respectively<sup>12</sup>), the decay profile of BaS:Eu powders is totally different. For BaS:Eu[0.1%] at room temperature, we determined two components with decay constants of approximately 10 and 140 ms, along with more persistent afterglow. This very slow decay compared to CaS:Eu and SrS:Eu points towards charge trapping phenomena, which incited us to perform thermoluminescence (TL) and excitation intensity dependent

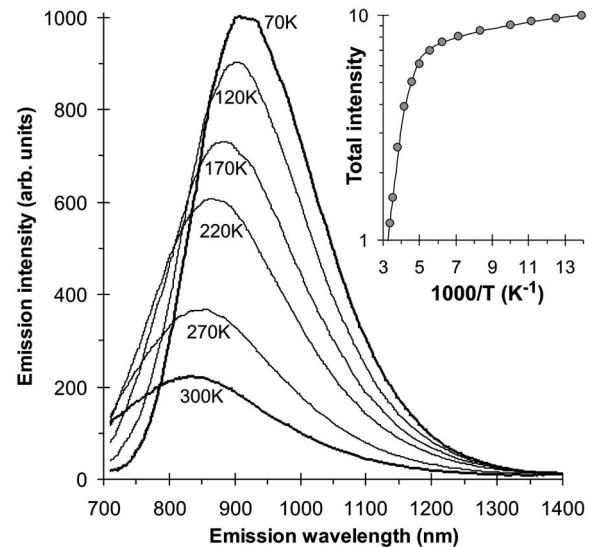


FIG. 2. Emission spectra of BaS:Eu[0.1%] as a function of measurement temperature. Excitation wavelength was 420 nm. The inset shows the Arrhenius plot of the total emission intensity, with the solid line a fit to the experimental data points, yielding activation energies of 14 and 190 meV.

measurements. Thermoluminescence measurements were performed by cooling the BaS:Eu powder to 70 K, followed by illumination in the  $t_{2g}$  excitation band (Ar laser at  $\lambda=488 \text{ nm}$ ). Then, the excitation light source was switched off and the sample was heated up with a controlled rate of 0.5 to 5 K/min while monitoring the light output at 775 nm. The TL could not be monitored at the peak emission wavelength as the dark current of the Ge detector was too high. Using the photomultiplier tube at 775 nm proved to be a good compromise between detector sensitivity and TL emission intensity. The TL spectra were appropriately corrected for the thermal quenching behavior and for the shift of the emission spectrum (see Fig. 2). The inset in Fig. 3 shows a typical TL spectrum for BaS:Eu[1.0%] powder. Beside a minor TL peak near room temperature, the main TL peak is situated around 200 K. To obtain a reliable value of the activation energy  $E$  associated with the main TL peak, Hoogenstraaten's heating rate method<sup>19</sup> was used. By variation of the heating rate  $\beta$ , the position of the maximum  $T_m$  of the TL peak changes according to the following formula (with  $s$  the frequency factor and  $k$  the Boltzmann's constant):

$$\frac{T_m^2}{\beta} = \frac{E}{sk} \exp\left(\frac{E}{kT_m}\right).$$

By using relatively low heating rates, temperature deviations between the sample and the temperature detector are minimized, which is essential for a reliable determination of the trap energy when using Hoogenstraaten's heating rate method.<sup>20</sup>

Based on the fitting shown in Fig. 3, a value of  $0.51 \pm 0.05 \text{ eV}$  was obtained for the activation energy. From these TL measurements, it is obvious that a large number of trap states will be empty at room temperature after the sample is kept in the dark for some time. Excitation of the

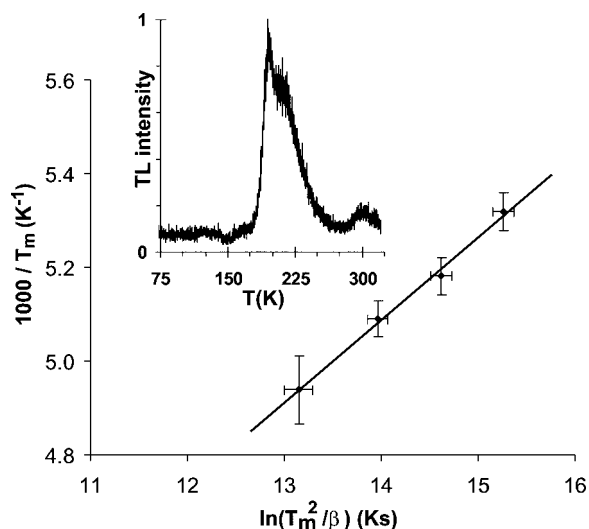


FIG. 3. Plot of  $1000/T_m$  as a function of  $\ln(T_m^2/\beta)$  for the determination of the trap energy by Hoogenstraaten's method, derived from TL measurements on BaS:Eu powder with heating rates of 0.5, 1.0, 2.0, and 5.0 K/min. The inset shows the TL intensity monitored at 775 nm as a function of temperature for BaS:Eu[1.0%]. A heating rate of 2.0 K/min was used.

BaS:Eu powder leads to a partial filling of these trap states, which is a process that competes with the light emission. After a certain time, a stationary condition is obtained and the emission intensity reaches a constant value. This effect is demonstrated in Fig. 4, where the light output is shown as a function of illumination time and excitation intensity. Prior to each measurement, the sample was kept in the dark for a sufficiently long time to allow the thermal emptying of the trap states. At low excitation intensities (typically  $0.1 \text{ mW/cm}^2$ ), it takes up to more than 1 min to reach a constant light output. At high excitation intensities

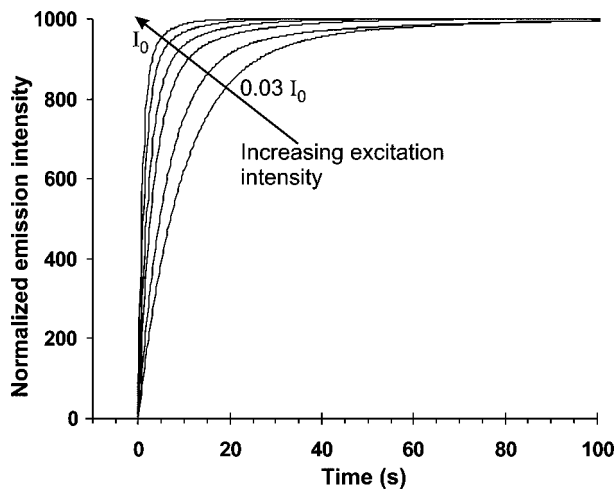


FIG. 4. Evolution of the light output of BaS:Eu[1%] powder at room temperature as a function of the excitation intensity (emission intensity monitored at 775 nm upon excitation at 425 nm). The evolution of the light output as a function of time was observed at 3%, 6%, 12%, 25%, 50%, and 100% of the highest excitation intensity  $I_0$  ( $2 \text{ mW/cm}^2$ ).

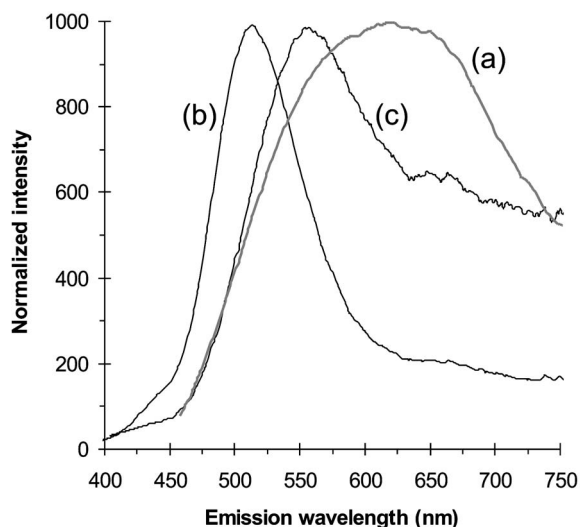


FIG. 5. Normalized emission spectra of undoped BaS powder (prepared by wet chemical synthesis) at an excitation wavelength of (a) 350 nm (RT), (b) 332 nm (70 K), and (c) 350 nm (70 K).

( $2 \text{ mW/cm}^2$ ), the trap states are almost immediately filled. Repeating this illumination experiment at 70 K immediately leads to a constant light output, as the trap states are not emptied when the powder is kept in the dark in between two measurements.

## B. Other emission bands

Beside the broad emission band peaking in the infrared for BaS:Eu<sup>2+</sup> powders, additional emission bands are detected in both europium-doped and undoped BaS powders. At room temperature, these emission bands are rather broad and very weak compared to the infrared emission band in BaS:Eu powders. As the bands are also present in undoped powders (prepared by sintering and by wet chemical synthesis), they are not related to Eu. Their relative intensity depends on the type of synthesis (sintering or wet chemical synthesis) and the synthesis temperature. Given the fact that the Eu<sup>2+</sup> emission in BaS:Eu is mainly situated in the deep red to infrared, the visual appearance of the powders under UV excitation is largely determined by these weak additional emission bands situated in the visible part of the spectrum. The emission appears yellow to orange-reddish at room temperature, depending on the excitation wavelength. At low temperature (70 K), several emission bands are partially resolved (Fig. 5).

Figure 6 shows the excitation spectrum monitored at 540 nm for undoped BaS powder, along with the excitation spectrum at 930 nm for BaS:Eu[0.1%], both measured at 70 K. For BaS:Eu, the excitation through the host (at wavelengths shorter than 325 nm) is less efficient than the direct transition in the Eu<sup>2+</sup> ion (in the wavelength range from 400 to 550 nm), similar to the case of CaS:Eu and SrS:Eu [Fig. 6(b)]. The dips at 309 and 320 nm have been previously reported in BaS powders and thin films,<sup>21,22</sup> and are related to the loss of excitation energy by surface reflection. They are assigned to the direct exciton transitions at the X point in

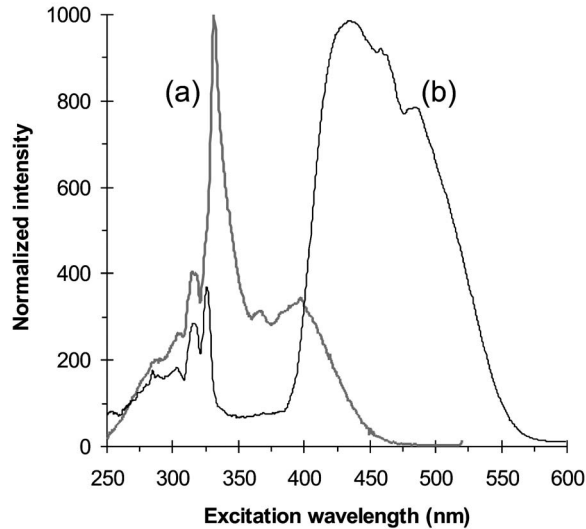


FIG. 6. Normalized excitation spectra at 70 K of (a) undoped BaS powder (prepared by wet chemical synthesis) at an emission wavelength of 540 nm and (b) of BaS:Eu[0.1%] at an emission wavelength of 930 nm.

the Brillouin zone.<sup>23,24</sup> The additional visible emission bands are mainly excited in the range from 325 to 425 nm, with excitation maxima at 332, 370, and 400 nm [Fig. 6(a)].

### C. Electron paramagnetic resonance

Eu<sup>3+</sup> ions cannot be detected with EPR, as the  $4f^6(^7F_0)$  ground state is nonmagnetic ( $J=0$ ). Eu<sup>2+</sup> on the other hand is easily detected, even at room temperature. The two isotopes <sup>151</sup>Eu and <sup>153</sup>Eu (natural abundancies of 47.8% and 52.2%, respectively) have a nuclear spin  $I=5/2$  (nuclear  $g_n$  factors of 1.39 and 0.61, respectively), which leads to a  $2 \times 6$  lines hyperfine structure on each EPR transition. In a cubic crystal field, the spin Hamiltonian for each isotope is given by<sup>25</sup> ( $S=7/2$ )

$$\hat{H} = g\mu_B \vec{B} \cdot \hat{S} + [B_4(\hat{O}_4^0 + 5\hat{O}_4^4) + B_6(\hat{O}_6^0 - 21\hat{O}_6^4)] + A\hat{S} \cdot \hat{I},$$

where the first term represents the Zeeman interaction (isotropic  $g$ ); the term between brackets is the zero-field splitting in which  $\hat{O}_k^m$  represents the Stevens operators; and the third

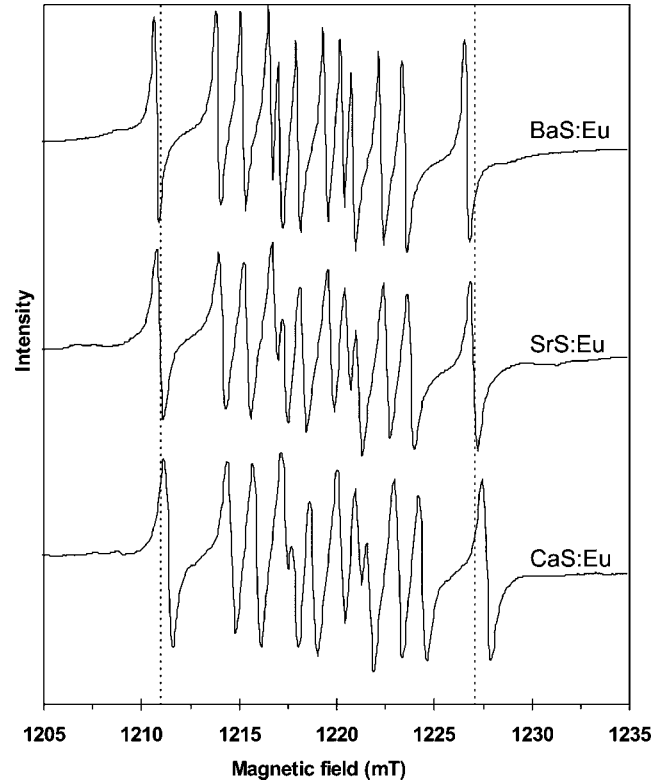


FIG. 7. Q band EPR spectra for CaS:Eu, SrS:Eu, and BaS:Eu at room temperature. Powders were prepared by sintering and dopant concentration was 0.1%. The dotted lines are a guide to the eye.

term is the hyperfine interaction (isotropic hyperfine constant  $A$ ). In a powder spectrum, usually only the angular independent  $M_S: \frac{1}{2} \rightarrow -\frac{1}{2}$  transition can be observed, from which the parameters  $g$  and  $A$  can be determined.

An overview of available literature data ( $g$  and  $A$ ) on europium-doped alkaline earth sulfides, mostly from the 1950's and 1960's, is reported in Table III. Error margins were not reported for most of the results; furthermore, Mn contamination often obscured the Eu signal. For comparison, data on the analogous alkaline earth oxides are given as well.

Figure 7 shows the  $Q$  band EPR spectra for Eu-doped alkaline earth sulfides (dopant concentration 0.1%). The spectra are very similar for the three compounds studied. Based on these spectra, values for  $g$  and  $A$  were obtained

TABLE III.  $g$  and  $A$  (for <sup>151</sup>Eu) for europium-doped alkaline earth sulfides and oxides.

Material	$g$	$A(^{151}\text{Eu})$ (MHz)	References
CaO:Eu	1.993	89.04	26
CaO:Eu	1.9918	90.42	27
SrO:Eu	1.991	89.64	28
BaO:Eu	1.9915	88.74	28
CaS:Eu	1.99	91.08	29
SrS:Eu	1.992+/-0.001	89.9+/-0.3	30
CaS:Eu	1.9902+/-0.0004	90.94+/-0.08	This work
SrS:Eu	1.9910+/-0.0004	89.96+/-0.08	This work
BaS:Eu	1.9913+/-0.0004	89.02+/-0.08	This work

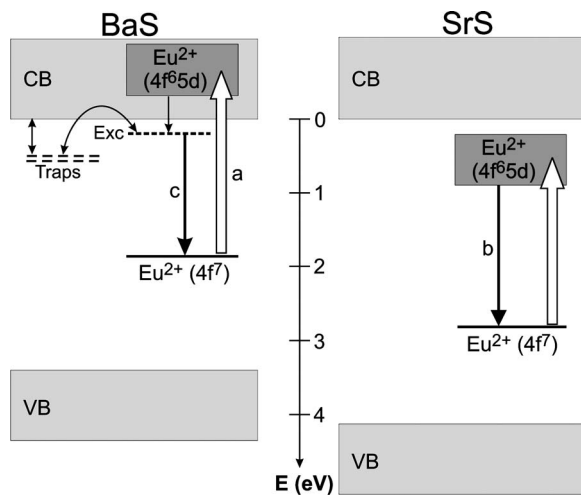


FIG. 8. Energy level scheme for BaS:Eu<sup>2+</sup> and SrS:Eu<sup>2+</sup>, with the ground and excited state for Eu<sup>2+</sup>, the conduction band (CB) and valence band (VB), the exciton level (Exc), and the trap levels. The transitions *a*, *b*, and *c* are referred to in the text.

using the EasySpin program package<sup>31</sup> and shown in Table III. They are in line with the few earlier reports on CaS:Eu and SrS:Eu. A systematic decrease in the hyperfine value is observed when going from CaS:Eu to BaS:Eu, which is similar to the analogous oxides.

## V. DISCUSSION

### A. Anomalous emission

With the data presented in Sec. IV A, the luminescence in BaS:Eu powders can indeed be called anomalous as all requirements proposed by Dorenbos are met: BaS:Eu shows a very large Stokes shift, a large FWHM of the emission band, and a deviating temperature quenching and decay profile upon comparison to the related materials CaS:Eu and SrS:Eu. This anomalous emission is explained by the *5d* excitation level being located near the host material's conduction band (Fig. 8). Upon excitation of a Eu<sup>2+</sup> ion (Fig. 8, transition *a*), it becomes autoionized and an impurity trapped exciton is created. A subsequent transition to the Eu<sup>2+</sup> ground state (Fig. 8, transition *c*) leads to a spectrum deviating from the anticipated emission as it is strongly redshifted.

Normal emission is obtained when the Eu<sup>2+</sup> excited state lies well below the conduction band (transition *b* in Fig. 8, shown for SrS:Eu<sup>2+</sup>). In this case, there is no low-energy crossing possible between the Eu<sup>2+</sup> excited state and the conduction band or exciton levels. In Refs. 9 and 32 configuration coordinate diagrams can be found for the emission in SrF<sub>2</sub>:Eu<sup>2+</sup> (showing normal emission) and BaF<sub>2</sub>:Eu<sup>2+</sup> (showing anomalous emission).

In the specific case of BaS:Eu, several trap levels are situated near the conduction band edge, as we observed in the thermoluminescence measurements. The main TL peak near 200 K corresponds to an activation energy of 0.51 eV. At room temperature, these trap levels (along with other trap levels) are slowly emptied when the BaS:Eu powder is placed in the dark after excitation. As this process partly

results in light emission, it explains the long decay constants and the afterglow. With this information, the evolution of the light output as a function of the excitation intensity can also be understood (see Fig. 4) as the preferential filling of the trap states. Eventually, a stationary condition is obtained and the light output becomes constant. As the number of traps is limited, a higher excitation intensity leads to a faster filling of the trap states.

In the case when the bottom of the *5d* level is located close to the bottom of the conduction band, it remains possible for the expected normal emission band to emerge at low temperature. However, in BaS:Eu this is not the case down to 70 K as no additional emission band emerged in the visible part of the spectrum. Hence we can conclude that the bottom of the *5d* level is well above the Eu<sup>3+</sup> trapped exciton level, and possibly situated in the conduction band (Fig. 8). On the basis of a configuration coordinate diagram, Dorenbos showed that a *5d* excited state could be located above the bottom of the conduction band, while the anomalous emission can still be present.<sup>9</sup> However, the anomalous emission can also occur when the lowest *5d* state is situated between the exciton level and the bottom of the conduction band. Based on our experiments it is not possible to determine the exact position of *5d* levels relative to the conduction band. Consequently, Fig. 8 illustrates only the possibility that the *5d* levels are entirely situated in the conduction band and no absolute position of the *5d* levels should be derived from it.

In general, anomalous emission does not arise randomly in rare earth doped phosphor materials. Dorenbos highlighted several trends for this anomalous emission to be present. In Eu<sup>2+</sup> doped compounds, it occurs more often when the Eu<sup>2+</sup> ion is substituted for a larger cation. Hence, anomalous emission is more common in barium compounds than in calcium or strontium compounds,<sup>9</sup> and has indeed also been observed in BaF<sub>2</sub>:Eu<sup>2+</sup> but not in SrF<sub>2</sub>:Eu<sup>2+</sup> (and CaF<sub>2</sub>:Eu<sup>2+</sup>).

It is tempting to try to explain this anomalous emission by arguing that it results from an incorporation of the Eu<sup>2+</sup> ions in BaS that is radically different from the case in CaS or SrS. In the latter materials, the Eu<sup>2+</sup> resides on regular Ca<sup>2+</sup> or Sr<sup>2+</sup> positions. Supposing the location of Eu<sup>2+</sup> in BaS is different, these Eu<sup>2+</sup> ions should experience a much higher value of the crystal field to explain the infrared emission as arising from a *4f<sup>6</sup>5d-4f<sup>7</sup>* transition. However, this hypothesis can be rejected for two reasons. First of all, the excitation spectrum for BaS:Eu is very similar to the two isomorphous materials and slightly shifted to higher energy as can be expected from a lower crystal field in BaS. Secondly, the normal incorporation of Eu in the BaS lattice is supported by the EPR spectra shown in Sec. IV C. In view of the low dopant concentration and of the assignment for Eu<sup>2+</sup> centers in other alkaline earth oxide and sulfides which present similar EPR spectra, we may assume that the majority of the Eu<sup>2+</sup> ions are incorporated on regular Ba<sup>2+</sup> positions of octahedral symmetry in BaS. The EPR data do not present evidence for incorporation at other (e.g., interstitial) sites. This further supports our hypothesis that the anomalous emission is related to the position of the Eu<sup>2+</sup> *5d* level in the conduction band of the BaS host lattice.

Concerning the thermal quenching behavior (Fig. 2), Dorenbos recently argued that the thermal quenching of the

$\text{Eu}^{2+}$   $5d$ - $4f$  luminescence in inorganic compounds is not related to the thermal release of a hole from the  $\text{Eu}^{2+}$  ground state to the valence band, nor to a large displacement between the ground and excited states of  $\text{Eu}^{2+}$  in the configuration coordinate diagram.<sup>33</sup> Instead, the thermal quenching is caused by the proximity of the  $5d$  excited level to the conduction band. Upon excitation (transition *a* in Fig. 8) to the  $4f^65d$  state of  $\text{Eu}^{2+}$ , the formation of an impurity trapped exciton is more probable than a transition to the conduction band levels, as motivated by Dorenbos using a configuration coordinate diagram.<sup>9</sup> From this exciton level, the infrared emission can occur (transition *b* in Fig. 8), while transitions to the conduction band states are likely to increase the chance of nonradiative decay. The activation energy of 190 meV determined from the Arrhenius plot in Fig. 2 (showing the thermal quenching profile) is ascribed to the dissociation of the impurity trapped exciton, which indeed increases the chance of nonradiative emission via the conduction band. The activation energy of 14 meV, which is about one tenth of the exciton dissociation energy, can then be related to the exciton binding energy.<sup>34</sup> The occurrence of a low thermal quenching temperature and the presence of anomalous, redshifted luminescence in BaS:Eu is also consistent with the trend Dorenbos observed in Ref. 33 for  $\text{Eu}^{2+}$ -doped MS and  $\text{MF}_2$  compounds, with  $M=\text{Ca}, \text{Sr}, \text{Ba}$ .

In the studied BaS:Eu powders, no  $\text{Eu}^{3+}$  line emission was detected. However, several reports have been made about  $\text{Eu}^{3+}$  line emission in EL devices (see Sec. II B). Although it was suggested that this could be due to the formation of Eu complexes<sup>16</sup> as the dopant concentration was rather high, ionization of the  $\text{Eu}^{2+}$  centers under high electrical fields applied in thin film electroluminescence could also play a role in the emission.

### B. Other emission bands

As stated in Sec. II B, several emission bands have been reported in the past for BaS:Eu<sup>2+</sup>. We showed in this work that the  $\text{Eu}^{2+}$  emission is situated in the infrared, but that several other weak emission bands can be observed in the visible part of the spectrum. As these bands also appear in purposely undoped BaS powders, they are related to impurities or intrinsic defects. For the analogous materials CaS and SrS, only a few studies have been devoted to the emission properties of undoped powders and thin films. Depending on the preparation condition, several emission bands were observed in the range from 340 to 590 nm and tentatively assigned to cation or anion vacancies, or trace impurities.<sup>24,35</sup>

In CaS and SrS nanoparticles, emission bands were observed at 460 and 545 nm, respectively.<sup>36</sup> Dedicated studies are required to pursue a similar assignment between the observed emission bands in BaS and intrinsic host defects or impurities. The presence of several energy levels just below the optical band gap of BaS, as observed in the excitation spectra for the emission bands in the visible part of the spectrum, could play a role in the emission mechanism of europium-doped BaS. Although these energy levels are not active for the  $\text{Eu}^{2+}$  emission in BaS:Eu [Fig. 6(b)], they could be related to the trap levels discussed above.

Nevertheless, it is important to keep in mind that the emission intensity of these bands is several orders of magnitude lower than the  $\text{Eu}^{2+}$  emission intensity. However, as the  $\text{Eu}^{2+}$  emission is mainly situated in the infrared, the visual appearance is largely determined by these additional bands. This can explain the often contradictory reports on the emission properties of BaS:Eu, as appropriate (i.e., infrared sensitive) detectors are required to observe the  $\text{Eu}^{2+}$  emission in BaS:Eu in the first place.

## VI. CONCLUSIONS

In this work, the emission properties of europium-doped BaS powders were explored and compared to the scarce and often contradictory literature data. At room temperature, the photoluminescence is characterized by a broad emission band peaking at 878 nm and by a large Stokes shift, which clearly deviates from the isomorphous compounds CaS:Eu and SrS:Eu. This anomalous emission, in combination with thermal quenching behavior and the decay profile, is related to the position of the  $5d$  excited level of  $\text{Eu}^{2+}$  relative to the conduction band levels of the host material. Thermoluminescence spectra point at a trap level with an activation energy of  $0.51 \pm 0.05$  eV. Beside the mainly infrared emission in BaS:Eu, additional weak emission bands in the visible part of the spectrum are described and assigned to the host material or to intrinsic defects. No line emission originating from  $\text{Eu}^{3+}$  was detected. EPR and PLE data suggest that  $\text{Eu}^{2+}$  ions in BaS are incorporated on regular  $\text{Ba}^{2+}$  positions of octahedral symmetry.

## ACKNOWLEDGMENTS

P.F.S. and J.V.H. wish to thank the BOF-UGent for financial support. H.V. acknowledges financial support from the Research Foundation-Flanders (FWO-Vlaanderen). This research is partially sponsored by FWO-Vlaanderen.

\*Email address: philippe.smet@ugent.be

<sup>1</sup>S. Shionoya and W. M. Yen, *Phosphor Handbook* (CRC Press, Boca Raton, 1999).

<sup>2</sup>R. P. Rao, *Mater. Res. Bull.* **21**, 249 (1986).

<sup>3</sup>N. Yamashita, *Jpn. J. Appl. Phys., Part 1* **30**, 3335 (1991).

<sup>4</sup>N. Miura, M. Kawanishi, H. Matsumoto, and R. Nakano, *Jpn. J. Appl. Phys., Part 2* **38**, L1291 (1999).

<sup>5</sup>R. B. Jabbarov, C. Chartier, B. G. Tagiev, O. B. Tagiev, N. N. Musayeva, C. Barthou, and P. Benalloul, *J. Phys. Chem. Solids* **66**, 1049 (2005).

<sup>6</sup>Y. Nakanishi, F. Shiba, K. Sowa, H. Tatsuoka, H. Kuwabara, T. Nakamura, and Y. Hatanaka, *Appl. Surf. Sci.* **100**, 639 (1996).

<sup>7</sup>Y. Nakanishi, H. Nakajima, N. Uekura, H. Kominami, M. Kottaisamy, and Y. Hatanaka, *J. Electrochem. Soc.* **149**, H165

- (2002).
- <sup>8</sup>P. Dorenbos, *J. Lumin.* **104**, 239 (2003).
- <sup>9</sup>P. Dorenbos, *J. Phys.: Condens. Matter* **15**, 2645 (2003).
- <sup>10</sup>D. S. McClure and C. Pedrini, *Phys. Rev. B* **32**, 8465 (1985).
- <sup>11</sup>H. Kasano, K. Megumi, and H. Yamamoto, *J. Electrochem. Soc.* **131**, 1953 (1984).
- <sup>12</sup>N. Yamashita, O. Harada, and K. Nakamura, *Jpn. J. Appl. Phys., Part 1* **34**, 5539 (1995).
- <sup>13</sup>P. Dorenbos, *J. Phys.: Condens. Matter* **15**, 4797 (2003).
- <sup>14</sup>J. E. Van Haecke, P. F. Smet, and D. Poelman, *Spectrochim. Acta, Part B* **59**, 1759 (2004).
- <sup>15</sup>J. Ihanus, T. Hänninen, T. Hatanpää, M. Ritala, and M. Leskelä, *J. Electrochem. Soc.* **151**, H221 (2004).
- <sup>16</sup>C. M. Maddix, Master thesis, Oregon State University, 2000.
- <sup>17</sup>P. F. Smet, D. Poelman, and R. L. Van Meirhaeghe, *J. Appl. Phys.* **98**, 184 (2004).
- <sup>18</sup>P. F. Smet, J. Van Gheluwe, D. Poelman, and R. L. Van Meirhaeghe, *J. Lumin.* **104**, 145 (2003).
- <sup>19</sup>W. Hoogenstraaten, *Philips Res. Rep.* **13**, 515 (1958).
- <sup>20</sup>T. M. Pitters, R. Melendrez, and W. Drozdowski, *Radiat. Prot. Dosim.* **84**, 127 (1999).
- <sup>21</sup>R. J. Zollweg, *Phys. Rev.* **111**, 113 (1958).
- <sup>22</sup>P. F. Smet, J. E. Van Haecke, R. L. Van Meirhaeghe, and D. Poelman, *J. Appl. Phys.* **98**, 043512 (2005).
- <sup>23</sup>A. Pourghazi and M. Dadsetani, *Physica B* **370**, 35 (2005).
- <sup>24</sup>R. Pandey and S. Sivaraman, *J. Phys. Chem. Solids* **52**, 211 (1991).
- <sup>25</sup>A. Abragam and B. Bleaney, *Electron Paramagnetic Resonance of Transition Ions* (Clarendon Press, Oxford, 1970), pp. 335–341.
- <sup>26</sup>N. Yamashita, *J. Electrochem. Soc.* **140**, 840 (1993).
- <sup>27</sup>A. J. Shuskus, *Phys. Rev.* **127**, 2022 (1962).
- <sup>28</sup>J. Overmeyer and R. J. Gambino, *Phys. Lett.* **9**, 108 (1964).
- <sup>29</sup>M. Pham-Thi, N. Ruelle, E. Tronc, D. Simons, and D. Vivien, *Jpn. J. Appl. Phys., Part 1* **33**, 1876 (1994).
- <sup>30</sup>A. A. Manenkov and A. M. Prokhorov, *Sov. Phys. Dokl.* **1**, 196 (1956).
- <sup>31</sup>S. Stoll and A. Schweiger, *J. Magn. Reson.* **178**, 42 (2006).
- <sup>32</sup>B. Moine, C. Pedrini, and C. Courtois, *J. Lumin.* **50**, 31 (1991).
- <sup>33</sup>P. Dorenbos, *J. Phys.: Condens. Matter* **17**, 8103 (2005).
- <sup>34</sup>A. M. Stoneham, *Theory of Defects in Solids, Electronic Structure of Defects in Insulators and Semiconductors* (Clarendon Press, Oxford, 1975), pp. 829–843.
- <sup>35</sup>A. N. Gruzintsev, V. T. Volkov, and A. N. Pronin, *J. Cryst. Growth* **117**, 975 (1992).
- <sup>36</sup>C. R. Wang, K. B. Tang, Q. Yang, and Y. T. Qian, *J. Electrochem. Soc.* **150**, G163 (2003).